Complex variables-based approach for analytical evaluation of boundary integral representations of three-dimensional acoustic scattering

Fatemeh Pourahmadian, Sofia G. Mogilevskaya*

Department of Civil, Environmental & Geo-Engineering, University of Minnesota, Minneapolis, United States

ARTICLE INFO

ABSTRACT

The paper presents the complex variables-based approach for analytical evaluation of three-dimensional integrals involved in boundary integral representations (potentials) for the Helmholtz equation. The boundary element is assumed to be planar bounded by an arbitrary number of straight lines and/or circular arcs. The integrals are re-written in local (element) coordinates, while in-plane components of the fields are described in terms of certain complex combinations. The use of Cauchy–Pompeiu formula (a particular case of Bochner–Martinelli formula) allows for the reduction of surface integrals over the element to the line integrals over its boundary. By considering the requirement of the minimum number of elements per wavelength and using an asymptotic analysis, analytical expressions for the line integrals are obtained for various density functions. A comparative study of numerical and analytical integration for particular integrals over two types of elements is performed.

© 2014 Elsevier Ltd. All rights reserved.

1. Introduction

This paper extends the complex variables-based integration technique recently developed for three-dimensional potential and elastostatic problems [14] to three-dimensional acoustic scattering problems described by the Helmholtz equation in frequency domain. It is well-known that the solutions of the latter problems can be represented by certain integrals, or combinations of integrals, over the boundary of the domain of interest, see e.g. [1,5,7]. The unknown fields in such representations can be found by solving the so-called boundary integral equations. The Boundary Element Method (BEM), see e.g. [1,5,9], is a numerical technique for solving these equations. The technique leads to the discretized equations that involve the integrals over the boundary elements used to approximate the boundaries of the simulation domains. Analytical evaluation of the integrals is an attractive option since it leads to higher accuracy of the computation and to the reduction of its cost. This may also facilitate the use of fast methods [11,20] and can be utilized (along with other methods such as cubature method and nonlinear regularizing transformations, e.g. see [16]) to form a robust framework for evaluation of BEM integrals in a more general context.

Closed-form results for the integrals involved in integral representations of the potential and elasticity theories are reported in many publications, especially for two-dimensional problems with straight elements [3,10,13,22] and for three-dimensional problems with triangular and rectangular elements [2,12,15,17,18,21,23,24]. However, only few papers report analytical results for the BEM integrals in acoustic scattering. One of such papers [8] presents a semi-analytical approach to evaluate singular and near singular double integrals involved in Galerkin formulation for the Helmholtz equation. The method employs constant approximations for the basic functions and uses triangular boundary elements (in coplanar or parallel planes). Analytical expressions for these integrals are provided for the singular parts of the Helmholtz Green's functions that coincide with the kernels of a single- and double-layer potentials of the Laplace equation, while numerical integration is used for the remaining dynamic part. The method is based on an integration formula for homogeneous functions that reduce an integral over an N-dimensional domain into an integral over its boundary.

The analytical approach presented in [25] (for 3D wave propagation) and in [26] (for transient heat conduction) also deals with singular and hypersingular BEM integrals over planar elements. The approach employs rectangular elements and constant approximations for the unknowns and relies on the Fourier series representation for the Helmholtz fundamental solution. It is shown that the method leads to satisfactory results, however, the minimum required number of terms in the Fourier expansion may become large or

* Corresponding author. Tel.: +1 6126254810.
  E-mail address: mogil003@umn.edu (S.G. Mogilevskaya).

sensitive to some specific parameters. Also, the possibility of spatial contamination can be another drawback of the method.

Another somewhat relevant paper [28] reports analytical expressions for moment integrals in the diagonal fast multipole BEM to solve 3-D acoustic wave problems. The paper also employs constant approximation for the unknowns and triangular elements.

In the present paper we use the complex variables-based technique proposed in [14] to evaluate three-dimensional integrals in the BEM formulations related to the Helmholtz equation. The technique is based on the complex integral representations that reduce the area integrals to those over the element contour. To use these representations, various complex combinations of in-plane fields and geometrical parameters are formed. For polynomial approximations of density functions in the BEM formulations, the procedure allows for analytical integrations of all integrals (regular, singular, and hypersingular) over planar elements bounded not only by straight lines but also by circular arcs (and, possibly, by other simple curves).

The structure of the paper is as follows. In Section 2, we present real variables-based integral representations involved in typical BEM formulations for the Helmholtz equation. In Section 3, we review various complex notations for geometry and fields and introduce generic complex integral. In Section 4, this integral is reduced to a contour integral using Cauchy–Pompeiu integral representation. In Section 5, the closed form expressions for this integral over a straight segment and a circular arc are presented. In Section 6, comparative analyses of numerical and analytical integration for particular integrals over elements of two types are performed. The outcome of the present study is summarized in Section 7 and its implications are discussed.

2. Integral representations of acoustic scattering in $\mathbb{R}^3$

The time-harmonic scalar wave propagation is governed by the following Helmholtz equation:

$$\Delta u + k^2 u = 0, \quad u = u(\boldsymbol{x}, \omega) = \mathrm{Re}[u(\boldsymbol{x})e^{-\mathrm{i}\omega t}], \quad k = \omega/c, \tag{1}$$

where u is the scalar field variable that is a function of position $\boldsymbol{x} \in \mathbb{R}^3$ and frequency ω, k is the wave number, and c is the medium's sound speed. The typical boundary element method formulations in acoustics involve the following integrals over the boundary, e.g. [1–3]:

- Single-layer potential

$$\int_S \frac{1}{4\pi r} v(\boldsymbol{\zeta}) e^{\mathrm{i}kr} \, \mathrm{d}S_\zeta, \tag{2}$$

- Double-layer potential

$$\int_S w(\boldsymbol{\zeta}) \frac{\partial}{\partial \mathbf{n}(\boldsymbol{\zeta})} \left[\frac{1}{4\pi r} e^{\mathrm{i}kr} \right] \mathrm{d}S_\zeta, \tag{3}$$

- Adjoint double-layer potential

$$\frac{\partial}{\partial \mathbf{n}(\boldsymbol{x})} \int_S \frac{1}{4\pi r} v(\boldsymbol{\zeta}) e^{\mathrm{i}kr} \, \mathrm{d}S_\zeta, \tag{4}$$

- Hypersingular potential

$$\frac{\partial}{\partial \mathbf{n}(\boldsymbol{x})} \int_S w(\boldsymbol{\zeta}) \frac{\partial}{\partial \mathbf{n}(\boldsymbol{\zeta})} \left[\frac{1}{4\pi r} e^{\mathrm{i}kr} \right] \mathrm{d}S_\zeta, \tag{5}$$

where $r = |\boldsymbol{\zeta} - \boldsymbol{x}|$ is the distance between the boundary point $\boldsymbol{\zeta} \in S$ and the field point $\boldsymbol{x} \in \mathbb{R}^3$; $\mathbf{n}(\boldsymbol{\zeta})$ denotes the unit normal vector to the boundary at the point $\boldsymbol{\zeta}$, while $\mathbf{n}(\boldsymbol{x})$ is the normal vector to some plane containing the point $\boldsymbol{x}$; the two scalars $v(\boldsymbol{\zeta})$ and $w(\boldsymbol{\zeta})$ are the so-called density functions. Eq. (1) is automatically satisfied when u is described by one of the expressions of Eqs. (2)–(5), or their linear combinations.

3. Generic integral involved in potentials (2)–(5)

With reference to Fig. 1, S is a planar boundary element consisting of a regular domain bounded by a piece-wise smooth and oriented contour ∂S that does not intersect itself. The element (local) coordinates are indicated by $(\zeta_1, \zeta_2, \zeta_3)$ so that ζ_3 is directed along the normal vector $-\mathbf{n}(\boldsymbol{\zeta})$, whereas ζ_1 and ζ_2 are in-plane directions chosen in such a way that $(\zeta_1, \zeta_2, \zeta_3)$ is a right handed coordinate system. Furthermore, assume that z is the projection of the field point $\boldsymbol{x}$ onto the element's plane. It should be mentioned that direction of travel on ∂S is assumed to be counter-clockwise.

As in [14], we employ the following complex combinations:

$$\begin{aligned} z &= x_1 + \mathrm{i}x_2, \quad \overline{z} = x_1 - \mathrm{i}x_2, \\ \tau &= \zeta_1 + \mathrm{i}\zeta_2, \quad h = \zeta_3 - x_3, \end{aligned} \tag{6}$$

wherein z, $\overline{z}$ – also τ, $\overline{\tau}$ – are hereafter treated as independent variables. Using these combinations, the distance r is expressed as follows:

$$r = \sqrt{(\tau - z)(\overline{\tau} - \overline{z}) + h^2}. \tag{7}$$

In the following we would also use the Wirtinger calculus,

$$\frac{\partial}{\partial z} = \frac{1}{2}\left[\frac{\partial}{\partial x_1} - \mathrm{i}\frac{\partial}{\partial x_2} \right], \quad \frac{\partial}{\partial \overline{z}} = \frac{1}{2}\left[\frac{\partial}{\partial x_1} + \mathrm{i}\frac{\partial}{\partial x_2} \right]. \tag{8}$$

The use of Eqs. (6)–(8) and the chain differentiation rule leads to the following useful interrelations:

$$r_{,1} = \frac{\partial r}{\partial z} + \frac{\partial r}{\partial \overline{z}}, \quad r_{,2} = \mathrm{i}\left(\frac{\partial r}{\partial z} - \frac{\partial r}{\partial \overline{z}} \right), \quad r_{,3} = -\frac{\partial r}{\partial h}, \tag{9}$$

where $r_j = \partial r/\partial x_j$.

In this setting, polynomial approximations of the density functions $v(\boldsymbol{\zeta})$, $w(\boldsymbol{\zeta})$ result in linear combinations of the terms $(\tau - z)^m(\overline{\tau} - \overline{z})^n$, e.g. the monomial $(\zeta_1)^2$ transforms to the following
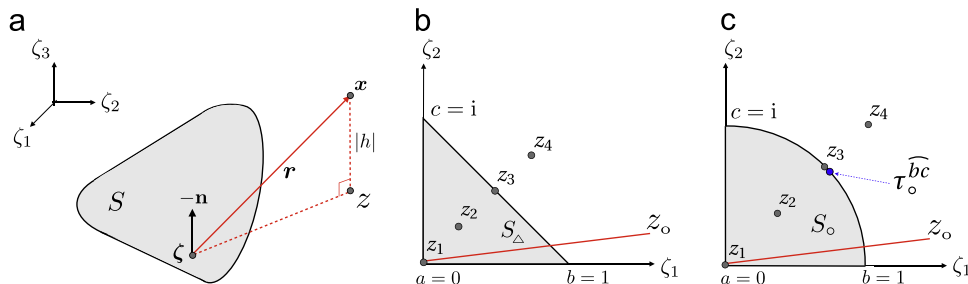
Fig. 1. Planar boundary elements: (a) typical element, (b) triangular element, (c) circular sector.
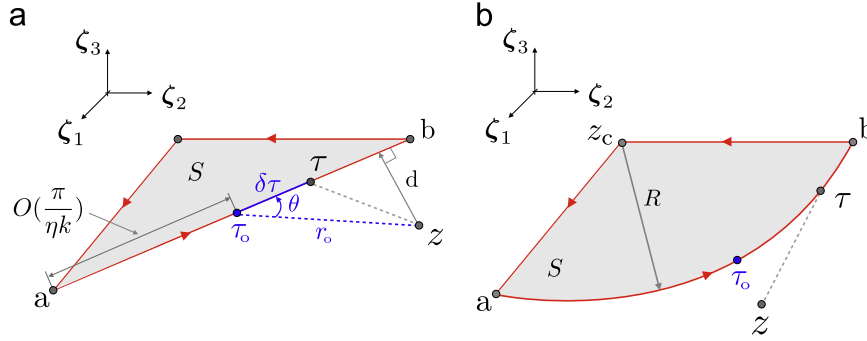
Fig. 2. A segment of a boundary element contour: (a) straight line, (b) circular arc.

expression:

$$(\zeta_1)^2 = \tfrac{1}{4}[(\tau-z)^2 + (\overline{\tau}-\overline{z})^2 + 2(\tau-z)(\overline{\tau}-\overline{z})$$
$$+ 2(\tau-z)(\overline{z}+z) + 2(\overline{\tau}-\overline{z})(\overline{z}+z) + (\overline{z}+z)^2], \qquad (10)$$

in which $z, \overline{z}$ are treated as parameters. Similar expressions exist for all other monomials.

Using expressions (6)–(9) and the expressions for the monomial of the types given by Eq. (10), one can show that, in the local coordinate system of the element S, all integrals involved in Eqs. (2)–(5) can be reduced to one generic integral of the form (note that z and $\overline{z}$ are now interpreted as parameters)

$$\int_S \frac{(\tau-z)^m(\overline{\tau}-\overline{z})^n}{r} e^{ikr} \, \mathrm{d}S, \quad m, n = 0, 1, \ldots, \qquad (11)$$

and its partial derivatives of various orders with respect to $z, \overline{z}, h$, and k.

4. Evaluation of the generic integral using complex integral representation

Following [14], we employ the Cauchy–Pompeiu integral representation (see e.g. [19,27]) and combine it with the Sokhotsli–Plemelj formulae for the limiting process as $z \to z_0 \in \partial S$. As a result, the area integral of Eq. (11) can be reduced to the contour integral as follows (to simplify expressions we excluded the constant wave number k from the list of parameters):

$$\mathcal{I}_{mn}(z, S) = \int_S \frac{(\tau-z)^m(\overline{\tau}-\overline{z})^n}{r} e^{ikr} \, \mathrm{d}S = \int_S \frac{1}{\tau-z} \frac{\partial f(\tau)}{\partial \overline{z}} \, \mathrm{d}S$$

$$= \frac{1}{2i} \int_{\partial S} \frac{f(\tau)}{\tau-z} \, \mathrm{d}\tau - \begin{cases} \pi f(z), & z \in S \\ \gamma f(z)/2, & z \in \partial S \\ 0, & z \notin S, \end{cases} \qquad (12)$$

where the contour integral is understood as the Cauchy principal value for $z \in \partial S$, and γ is the internal angle of element's edge at $z \in \partial S$ such that

$$\frac{\gamma}{2\pi} = \begin{cases} 1/2 & \text{at regular points} \\ 0 < \gamma_k \le 2 & \text{at } k\text{th corner point,} \end{cases} \qquad (13)$$

and the parameter z is excluded from the list of arguments of the function f for the sake of simplicity.

The function $f(\tau)$ of Eq. (12) can be represented as follows:

$$\frac{\partial f(\tau)}{\partial \overline{z}} = \frac{(\tau-z)^{m+1}(\overline{\tau}-\overline{z})^n}{r} e^{ikr}. \qquad (14)$$

In cases of constant, linear, and quadratic approximations of density functions, $f(\tau)$ of Eq. (14) can be expressed in the following closed form:

$$f(\tau) = \begin{cases} 2ik^{-1}(\tau-z)^m e^{ikr}, & n = 0 \\ 2ik^{-3}(\tau-z)^{m-1} e^{ikr}\left[-2 + 2ikr + k^2(r^2-h^2)\right], & n = 1 \\ 2ik^{-5}(\tau-z)^{m-2} e^{ikr}\left[24 + k\left(-8kh^2 - 24ir + k(r^2-h^2)(k^2(r^2-h^2) + 4ikr - 12)\right)\right] & n = 2. \end{cases} \qquad (15)$$

The free term on the right-hand side of Eq. (12) is evaluated by substituting $\tau = z$ in Eq. (15). Some examples are provided in Appendix A.

In this setting, we study the possibilities for analytical integration of the contour integral of Eq. (12) over the elements whose boundary ∂S consists of various combinations of straight segments or circular arcs.

5. Analytical integration for planar elements

5.1. Straight boundary segment

The complex representation of a straight segment with end points denoted by $a = a_1 + i\,a_2$ and $b = b_1 + i\,b_2$ (see Fig. 2(a)) results in the following expression for the conjugate variable $\overline{\tau}$ (see [10,13,14]):

$$\overline{\tau} = \overline{a} + D_{ab}(\tau - a), \qquad (16)$$

where

$$D_{ab} = \frac{\overline{b} - \overline{a}}{b - a}.$$

This allows for the description of the distance r in terms of the single variable τ

$$r = \sqrt{(\tau-z)(D_{ab}(\tau-z) + 2\overline{d}) + h^2}, \quad d = d_1 + id_2 = \tfrac{1}{2}(a - z - \overline{D}_{ab}(\overline{a} - \overline{z})). \qquad (17)$$

Note that $|d| = 0$ if $z \in [a, b]$, and $D_{ab} = -\overline{d}/d$ if $z \notin [a, b]$.

Eqs. (16) and (17) manifest path-dependency of the line integrals for non-holomorphic functions. Substitution of Eq. (15) into the contour integral of Eq. (12) leads to the following integral

over some straight segment $[a, b] \in \partial S$:

$$I_{pq}(z, a, b) = \int_{\ell_{ab}} r^p (\tau - z)^q \, e^{ikr} \, d\tau, \tag{18}$$

where ℓ_{ab} denotes the straight path from the point a to b. It can be shown by considering Eq. (17) that for constant, linear, and quadratic approximations, (p, q) are integers such that $p = 0, 1$; $-3 \leq q \leq 4$. The last step towards analytical evaluation of the integral of Eq. (18) stems from the following critical requirement. In order to avoid aliasing and other sources of wave-field misinterpretation, the boundary of the simulation domain must be discretized considering the

$$I_{pq}(z, a, b) = \begin{cases} -\dfrac{1}{2t^2 h^3} \left(hr(h^2 + \overline{d}t) + t^2(\overline{d}^2 - D_{ab}h^2) \ln\left[\dfrac{t}{h^2 + hr + t\overline{d}} \right] \right) \Big|_{\tau = a}^{\tau = b}, & q = -3, \\[4mm] -\left(\dfrac{r}{t} + \sqrt{D_{ab}} \ln\left[-\overline{d} - D_{ab}t + \sqrt{D_{ab}}\, r \right] - \dfrac{\overline{d}}{h} \ln\left[\dfrac{-t}{h^2 + hr + t\overline{d}} \right] \right) \Big|_{\tau = a}^{\tau = b}, & q = -2, \\[4mm] r + h \ln[t] + \dfrac{\overline{d}}{\sqrt{D_{ab}}} \ln\left[\overline{d} + D_{ab}t + \sqrt{D_{ab}}\, r \right] \Big|_{\tau = a}^{\tau = b}, & q = -1, \end{cases} \tag{23}$$

radiation frequency, so that the number of elements per wavelength is at least five to ten depending on the order of approximation. This implies that the oscillatory part of the kernel, e^{ikr}, in Eq. (18) over the support $[a, b]$ is a smooth and slowly varying function regardless of the frequency regime, as the element size scales down with the wavelength $\lambda = 2\pi/k$. Thus, thanks to the BEM discretization, the asymptotic approximation used in low frequency scattering [4] can be employed in the general context of arbitrary radiation frequency to describe e^{ikr} over $[a, b]$.

To this end, the distance r is expressed with respect to the mid-point $\tau_0 = (a + b)/2$ (see Fig. 2(a)) of the integration interval $[a, b]$ as follows ($\tau \in [a, b]$):

$$r = |\boldsymbol{\zeta} - \boldsymbol{x}| = \sqrt{r_o^2 + \delta\tau^2 - 2r_o\delta\tau \cos(\theta)},$$

$$r_o = |z - \tau_o| = \sqrt{(\tau_o - z)(D_{ab}(\tau_o - z) + 2\overline{d}) + h^2},$$

$$\delta\tau = |\tau - \tau_o| = O\left(\frac{\pi}{\eta k} \right), \tag{19}$$

where $\eta \geq 5$ is the number of elements per wavelength and θ is the angle between $z - \tau_o$ and $\tau - \tau_o$. Expanding the distance r of Eq. (19) into Taylor series with respect to $\delta\tau$, one obtains

$$\begin{cases} r = r_o - \cos(\theta)\delta\tau + \dfrac{\sin(\theta)^2}{2r_o}\delta\tau^2 + O(\delta\tau^3), & r_o > O(\delta\tau), \\[3mm] r = O(\delta\tau), & r_o \leq O(\delta\tau), \\[2mm] r = \delta\tau, & r_o = 0. \end{cases} \tag{20}$$

Consequently, as τ varies by $\delta\tau = O(\pi/(\eta k))$ about τ_o within the integration interval $[a, b]$, r varies around r_o by $\delta r = O(\delta\tau)$ provided r_o is sufficiently large, i.e. $r_o > O(\delta\tau)$. In the case where r_o approaches zero (say $r \leq O(\delta\tau)$), the total distance r scales as $O(\delta\tau)$. Whence, $k\delta r$ (or kr for small r_o) behaves like $O(\pi/\eta)$ for $\tau \in [a, b]$, which allows for the following asymptotic expansion:

$$e^{ikr} = e^{ikr_o}\left(1 + ik\delta r + \cdots + \frac{i^n}{n}(k\delta r)^n + \cdots \right), \quad \delta r = r - r_o,$$

$$\tau \in [a, b], \quad n = 0, 1, \ldots. \tag{21}$$

It is important to note that the right-hand side of Eq. (21) provides a rapidly convergent series representation even with the minimum required number of elements per wavelength, $\eta = 5$. As explained above, due to proper scaling via the BEM discretization procedure, the rate of convergence for the series does not depend on the frequency of wave propagation, or other parameters. In

Section 6, we show that the expansion produces highly accurate results even when it is truncated at the 5th–6th term. As a result of this asymptotic analysis, the integrals of Eq. (2)–(5) can be reduced to the integrals of the following forms:

$$I_{pq}(z, a, b) = \int_{\ell_{ab}} r^p (\tau - z)^q \, d\tau, \quad r = \sqrt{(\tau - z)(D_{ab}(\tau - z) + 2\overline{d}) + h^2}, \tag{22}$$

wherein $p = 0, 1$, $q \geq -3$ and ℓ_{ab} denotes the straight path from the point a to b. Analytical integration of Eq. (22) for $p = 1$ results in the following closed-form expressions:

in which the results corresponding to $q \geq 0$ are omitted since they are reported in [14] (see Eqs. (8.9), (8.11) of [14] for $q \geq 0$). The results for the case $p = 0$ are straightforward and, therefore, are not reported here. These results and expressions of Eq. (23) form a complete library of integrals necessary and sufficient for analytical integration of BEM representations in acoustic scattering over planar elements whose boundaries can be described by a set of straight segments.

5.2. Circular boundary segment

The complex equation associated with the circular arc $\widehat{ab}$ of radius R centered at z_c, shown in Fig. 2(b), is described by

$$(\overline{\tau} - \overline{z}_c)(\tau - z_c) = R^2, \quad z_c = (z_c)_1 + i(z_c)_2, \tag{24}$$

which allows for the following expression of the conjugated variable:

$$\overline{\tau} = \overline{z}_c + \frac{R^2}{\tau - z_c}. \tag{25}$$

Thus, the distance r can be expressed as a function of the single variable τ as follows:

$$r = \sqrt{(\tau - z)\left(\overline{z}_c - \overline{z} + \frac{R^2}{\tau - z_c} \right) + h^2}. \tag{26}$$

As in previous case, the path-dependency of the line integrals for non-holomorphic functions is expressed by Eqs. (24)–(26). Analytical evaluation of Eq. (18) over the circular arc $\widehat{ab}$ is carried out in the fashion described in Section 5.1 by invoking the same requirement on the minimum number of elements par wavelength η. The asymptotic expansion of e^{ikr} of Eq. (21) is employed wherein the center of expansion τ_o is the mid-arc point (see Fig. 2(b)). The procedure leads to the integrals of the following forms:

$$J_{pq}(z, a, b) = \int_{r_{ab}} r^p (\tau - z)^q \, d\tau, \quad p = 0, 1, \quad q \geq -3, \tag{27}$$

where r_{ab} denotes the circular path from the point a to b, and r is described by Eq. (26). The procedure of integrating Eq. (27) is as follows.

For the case of $z = z_c$, the distance r (for all $\tau \in \widehat{ab}$) becomes constant, i.e. $r = \sqrt{R^2 + h^2}$. Hence, $J_{pq}(z, a, b)$ of Eq. (27) reduces to a

Table 1
Comparison of numerical and analytical integration (triangular element) for $\eta = 5$.

$\mathcal{I}_{00}(z, S_{\triangle})$	$z_1 = 0$	$z_2 = 0.25 + 0.25i$	$z_3 = 0.5 + 0.5i$	$z_4 = 0.75 + 0.75i$
Numerical	$1.1444 + 0.4214i$	$2.3062 + 0.4330i$	$1.6866 + 0.4306i$	$0.6683 + 0.4145i$
Analytical	$1.1444 + 0.4214i$	$2.3103 + 0.4330i$	$1.6896 + 0.4306i$	$0.6683 + 0.4145i$
$E[\mathcal{I}_{00}(z, S_{\triangle})]$	0.01%	0.17%	0.17%	0.01%

set of elementary integrals [6] i.e.

$$J_{pq}(z_c, a, b) = (R^2 + h^2)^{p/2} \int_{r_{ab}} (\tau - z_c)^q \, d\tau$$

$$= \begin{cases} \dfrac{1}{q+1} (R^2 + h^2)^{p/2} (\tau - z_c)^{q+1} \Big|_{\tau = a}^{\tau = b}, & q \neq -1 \\[2mm] (R^2 + h^2)^{p/2} \ln(\tau - z_c) \Big|_{\tau = a}^{\tau = b}, & q = -1. \end{cases} \quad (28)$$

In the case of $z \neq z_c$, the change of variable $t = (\tau - z_c)/(z - z_c)$, remarkably simplifies the calculation procedure. In this case, r can be recast as

$$r = |z| \sqrt{\frac{g(t)}{t}}, \quad z = z_c - z, \quad z \neq z_c, \quad (29)$$

where the real variables function $g(t)$ is described by

$$g(t) = t^2 + At + B, \quad A = \frac{h^2 + R^2 + |z|^2}{|z|^2}, \quad B = \left(\frac{R}{|z|}\right)^2.$$

Also, for the future reference, the roots of $g(t) = 0$ which appear in the final expressions are denoted by

$$\chi_1 = \tfrac{1}{2}\left(A - \sqrt{A^2 - 4B}\right), \quad \chi_2 = \tfrac{1}{2}\left(A + \sqrt{A^2 - 4B}\right),$$

$$g(-\chi_1) = g(-\chi_2) = 0. \quad (30)$$

Considering Eq. (29), the integral of Eq. (27) can be recast as follows:

$$J_{pq}(z, a, b) = z^{q+1} |z|^p \int_{t_1}^{t_2} \left(\frac{t^2 + At + B}{t}\right)^{p/2} (t + 1)^q \, dt, \quad p = 0, 1, -3 \leq q, \quad (31)$$

where $t_1 = (a - z_c)/z$ and $t_2 = (b - z_c)/z$. The integrals associated with $p = 0$ in Eq. (27) are elementary integrals, so henceforth, the case $p = 1$ is considered. Moreover, the expressions corresponding to $p = 1$ and $q \geq 0$ have already been reported in [14] (see Eq. (8.17) of [14] for $n = 0$ and $m \geq 0$) and will not be reproduced here. The final expression for the case $p = 1$ and $q \leq 0$ has the following form:

$$J_{pq}(z, a, b) = z^{q+1} |z|^p \left(C_q^0 + C_q^1 E(t) + C_q^2 F(t) + C_q^3 P(t) \right) \Big|_{t_1 = (a - z_c)/z}^{t_2 = (b - z_c)/z}, \quad (32)$$

where $p = 1$, $-3 \leq q < 0$ and the coefficients C_q^s for $s = 0, \ldots, 3$ are as follows,

- $q = -1$:

$$C_q^0 = \frac{2r}{|z|}, \quad C_q^1 = 2i \sqrt{\chi_1}, \quad C_q^2 = 2i \sqrt{\chi_1}(\chi_2 - 1), \quad C_q^3 = \frac{2i\chi_3}{\sqrt{\chi_1}}, \quad (33)$$

- $q = -2$:

$$C_q^0 = -\frac{r}{|z|(1 + t)}, \quad C_q^1 = -i \sqrt{\chi_1}, \quad C_q^2 = i \sqrt{\chi_1}(\chi_2 + 1),$$

$$C_q^3 = -\frac{i(B - 1)}{\sqrt{\chi_1}}, \quad (34)$$

- $q = -3$:

$$C_q^0 = \frac{r(1 - 2A + 3B + (B - 1)t)}{4|z|\chi_3(1 + t)^2}, \quad C_q^1 = \frac{i\chi_1(1 - 2A + 3B)}{4\chi_3},$$

$$C_q^2 = -\frac{i\chi_1(\chi_2(\chi_4 - 2A + 4) + \chi_4)}{4\chi_3},$$

$$C_q^3 = \frac{i(B(5 - 2A + \chi_4) - 1)}{4\chi_3 \sqrt{\chi_1}}, \quad (35)$$

in which

$$E(t) = E\left(\sin^{-1}\left(i\sqrt{\frac{\chi_1}{t}}\right)\Big|\frac{\chi_2}{\chi_1}\right),$$

$$P(t) = \Pi\left(\frac{1}{\chi_1}; \sin^{-1}\left(i\sqrt{\frac{\chi_1}{t}}\right)\Big|\frac{\chi_2}{\chi_1}\right),$$

$$F(t) = F\left(\sin^{-1}\left(i\sqrt{\frac{\chi_1}{t}}\right)\Big|\frac{\chi_2}{\chi_1}\right), \quad \chi_3 = A - B - 1,$$

$$\chi_4 = 1 - 2A + 3B,$$

and $F(\phi|k)$, $E(\phi|k)$, and $\Pi(\ell; \phi|k)$ are elliptic integrals of first, second, and third kind defined as follows:

$$F(\phi|k) = \int_0^\phi \left(1 - k \sin^2 \theta\right)^{-1/2} d\theta,$$

$$E(\phi|k) = \int_0^\phi \left(1 - k \sin^2 \theta\right)^{1/2} d\theta,$$

$$\Pi(\ell; \phi|k) = \int_0^\phi \left(1 - \ell \sin^2 \theta\right)\left(1 - k \sin^2 \theta\right)^{-1/2} d\theta.$$

6. Comparison of analytical and numerical integration results

The performance of the proposed approach is investigated in this section. To this end, the generic integral of Eq. (11) is considered for some specific combinations of the parameters, $m = n = 0, 1, 2$. Then, the surface integrals over two specific planar elements shown in Fig. 1(b, c) are evaluated both analytically, based on the proposed method – whose associated closed-form solutions are provided in Appendix A – and, numerically, by applying Gaussian quadrature scheme which incorporates a large number of sampling points, so that the resulting values are exact up to eight decimal places. For numerical integration, the regularization procedure introduced in [1, Chapter 3] is implemented. First, the surface variables (ζ_1, ζ_2) are transformed to polar coordinates (ϱ, ϑ). Second, the Gaussian quadrature is used with (50×50) sampling points to evaluate the surface integrals. In the numerical experiments, the critical case $h = 0$ is considered and z is chosen to be located either along the ray Oz_o or at certain fixed points z_s, $z = 1, 2, 3, 4$ (see Fig. 1(b, c)). The number of terms η in asymptotic expansion Eq. (21) is intentionally set to be the minimum, i.e. $\eta = 5, 6$.

The comparison between the numerical and analytical results for the generic integral of Eq. (11) with $m = n = 0$ is reported in Table 1 for the triangular element. The same results for the circular sector are reported in Table 2. The locations of four specific field points are illustrated in Fig. 1(b, c). Moreover, the reported error is

Table 2
Comparison of numerical and analytical integration (circular sector) for $\eta = 6$.

$\mathcal{I}_{00}(z, S_\circ)$	$z_1 = 0$	$z_2 = 0.35 + 0.35i$	$z_3 = 0.7071 + 0.7071i$	$z_4 = 1.0 + 1.0i$
Numerical	$1.3758 + 0.6477i$	$2.9538 + 0.6778i$	$1.9662 + 0.6649i$	$0.7107 + 0.6222i$
Analytical	$1.3758 + 0.6477i$	$2.9561 + 0.6778i$	$1.9662 + 0.6649i$	$0.7107 + 0.6222i$
$E[\mathcal{I}_{00}(z, S_\circ)]$	0.01%	0.0762%	0.01%	0.01%
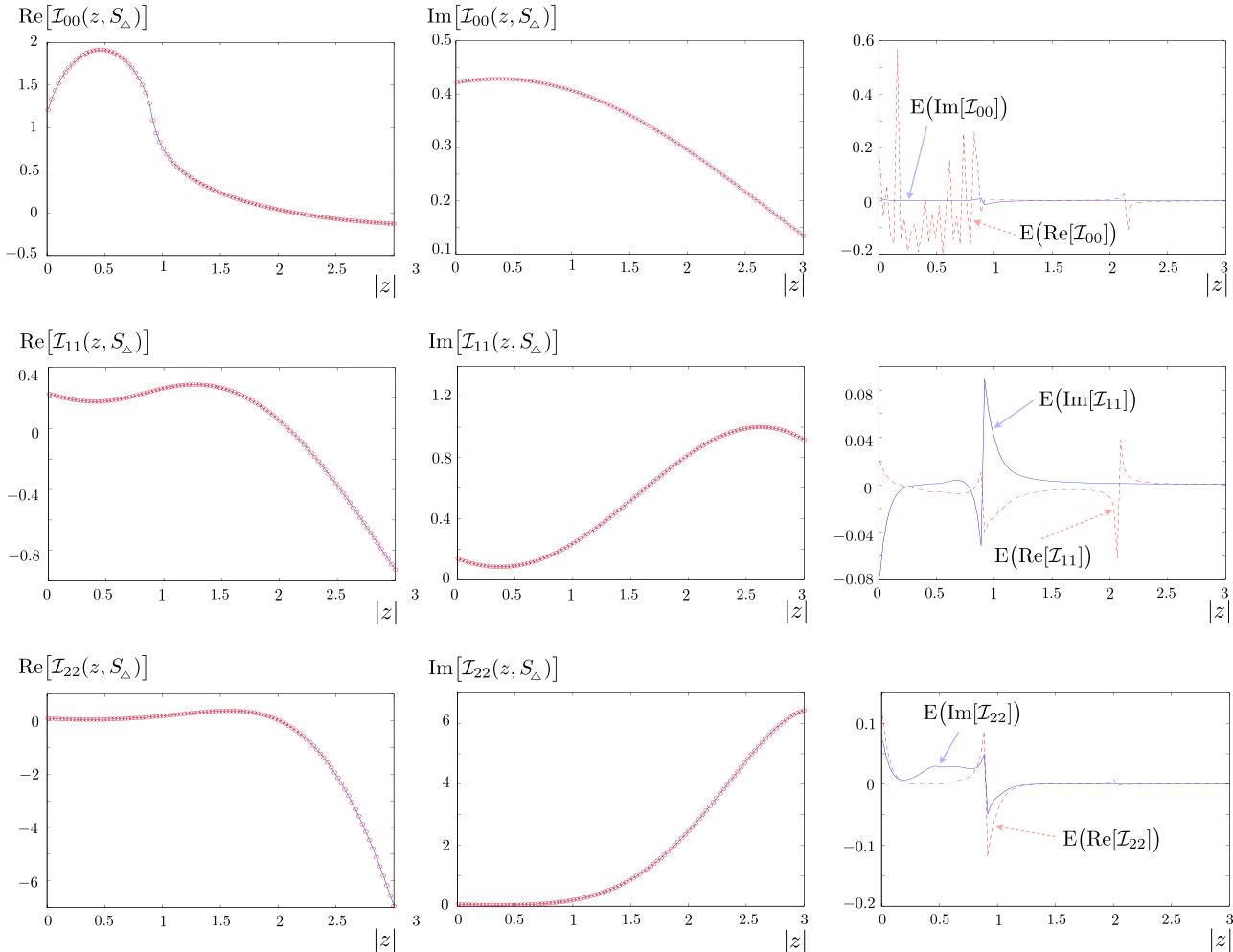
Fig. 3. Analytical (solid line) vs. numerical (circular dots) integration over $S_\triangle$ (depicted in Fig. 1(b)) and, its corresponding error percent for $\mathcal{I}_{mn}(z, S_\triangle)$ defined by Eq. (12) where $z \in Oz_\circ$ (see Fig. 1(b)).

calculated as follows:

$$E[\mathcal{I}_{mn}(z, S)] = 100 \times \frac{|\text{Num.}(\mathcal{I}_{mn})| - |\text{Anal.}(\mathcal{I}_{mn})|}{|\text{Num.}(\mathcal{I}_{mn})|}.$$

To observe the spacial variation, the integration is performed along the ray Oz_o and shown in Figs. 3 and 4 for three parameter combinations $m = n = 0$, $m = n = 1$, $m = n = 2$ (respectively rows one to three).

7. Concluding remarks

The approach presented in this paper allows for analytical evaluation of the basic integrals involved in three-dimensional integral representations for the Helmholtz equation. The boundary elements are considered to be planar, bounded by straight segments or, circular arcs, while the unknown fields are described using polynomial

approximation. The use of complex representation and complex analysis leads to the reduction of all the basic integrals to the generic integral and its derivatives with respect to specific parameters. The final closed-form expressions are achieved using proposed asymptotic expansion of the oscillatory part of the kernel in the generic integral. The expansion is based on the requirement of the minimum number of elements per wavelength. It is demonstrated that the series is rapidly convergent, and the rate of convergence does not depend on the frequency of wave propagation or any other parameters. The analytical results are compared to those obtained numerically using extensive number of Gauss points in the Gauss-Quadrature method. The numerical experiments showed that the generic integral can be accurately evaluated with reasonable computational effort for various planar elements. The proposed approach can be employed to create integration subroutines or functions that can be used as black boxes by the developers of the BEM-based software. We believe that the technique could be extended to elastodynamics in a straightforward
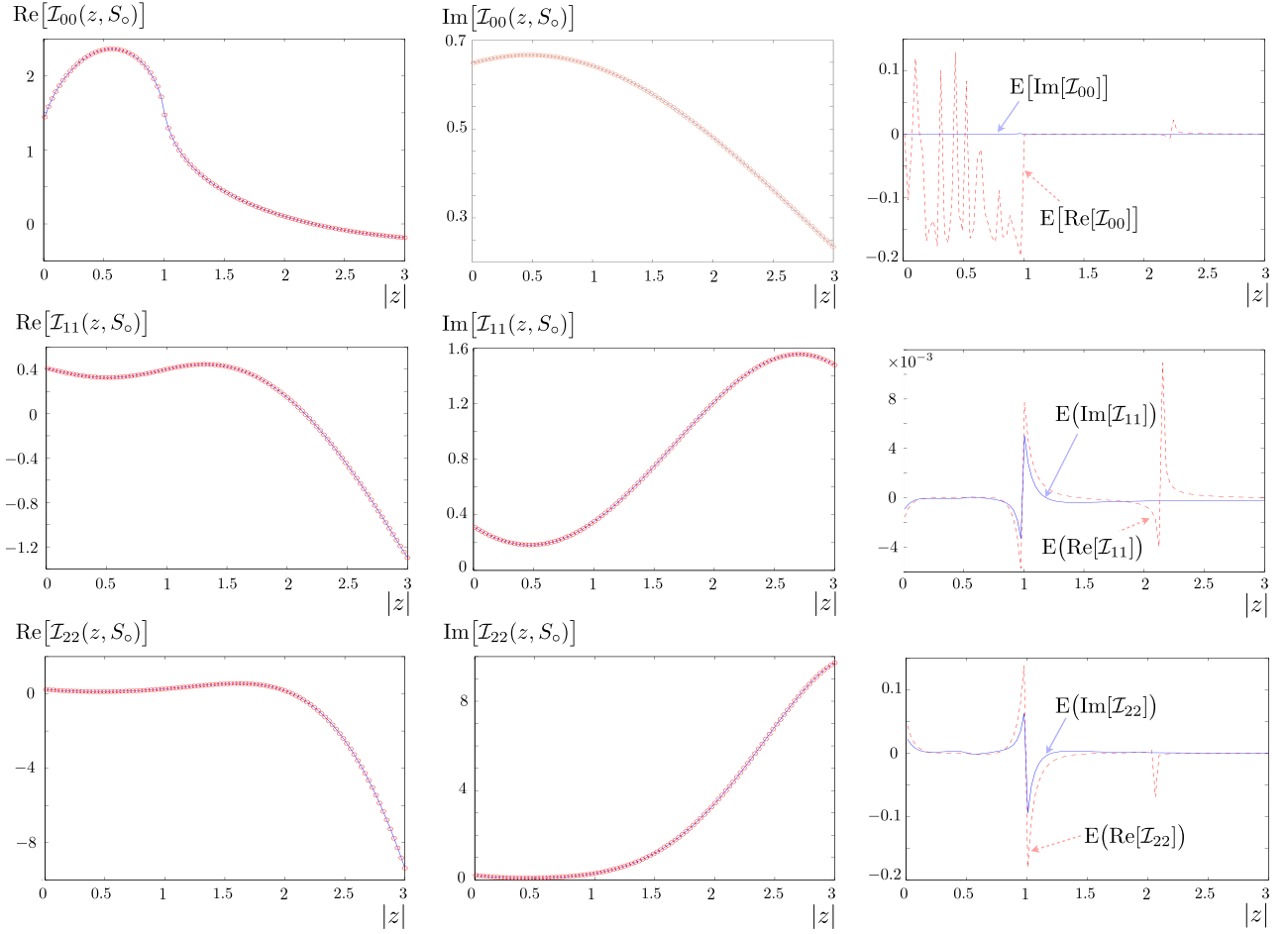
Fig. 4. Analytical (solid line) vs. numerical (circular dots) integration over $S_\circ$ (depicted in Fig. 1(c) and, its corresponding error percent for $\mathcal{I}_{mn}(z, S_\circ)$ defined by Eq. (12) where $z \in Oz_\circ$ (see Fig. 1(c)).

fashion. Using the method, it is effortless to adapt available codes developed for solving static problems to tackle dynamic problems by simply adding the new integrals introduced in this paper to the library of generic integrals. The analytical expressions obtained here for three-dimensional problems could be used for the area integrals associated with body force terms involved in the corresponding two-dimensional BEM formulations with non-zero body forces. They could also be useful in developing multipole expansions employed in fast multipole methods. The future work may include the use of non-planar (isoparametric) elements, as well as planar elements bonded by some other elementary curves. The use of different approximating functions for the unknowns could also be investigated.

Acknowledgment

Appendix A. Closed-form solution of $\mathcal{I}_{mn}(z, S_\triangle)$ and $\mathcal{I}_{mn}(z, S_\bigcirc)$

A.1. Analytical integration of $\mathcal{I}_{mn}(z, S_\triangle)$

To illustrate the implementation of the proposed method, the calculation procedure, and its results, analytical expressions of the integral $\mathcal{I}_{mn}$ reported in Table 1 and, Fig. 3, i.e. $m=n=0$, $m=n=1$, $m=n=2$, are presented below:

Evaluation of $\mathcal{I}_{00}(z, S_\triangle)$: In the case where $m=n=0$ and $z \notin S_\triangle$ where $S_\triangle$ is the right triangle shown in Fig. 1(b). Using Eqs. (12) and (15), the following identity is attained:

$$\mathcal{I}_{00}(z, S_\triangle) = \int_{S_\triangle} \frac{1}{r} e^{ikr}\, dS_\triangle = \frac{1}{k} \int_{\partial S_\triangle} \frac{e^{ikr}}{\tau - z}\, d\tau, \tag{A.1}$$

where the contour $\partial S_\triangle$ consists of linear segments ℓ_{ab}, ℓ_{bc} and ℓ_{ca} along with vertices $a=0$, $b=1$ and $c=i$. One should note that the free term of Eq. (12) vanishes when $z \notin S_\triangle$. In view of the asymptotic expansion for e^{ikr} in Eq. (21), the integral of Eq. (A.1) along the linear segment ℓ_{ab} can be recast as

$$\frac{1}{k} \int_{\ell_{ab}} \frac{e^{ikr}}{\tau - z}\, d\tau = e^{ik\, r_\circ^{ab}} \sum_{n=0}^{5} \frac{i^n k^{n-1}}{n!} \int_{\ell_{ab}} \frac{1}{\tau - z} (r - r_\circ^{ab})^n\, d\tau, \tag{A.2}$$

in which $r_\circ^{ab} = |z - \tau_\circ^{ab}|$, with $\tau_\circ^{ab}$ being the mid-point of segment ℓ_{ab}, i.e. $\tau_\circ^{ab} = (a+b)/2$. By substituting the well-known binomial theorem

$$(r - r_\circ^{ab})^n = \sum_{m=0}^{n} \frac{n!}{m!(n-m)!} (-r_\circ^{ab})^{n-m}\, r^m, \quad 5 \geq n \geq 0, \tag{A.3}$$

into Eq. (A.2), and performing similar calculations for the remaining segments ℓ_{bc} and ℓ_{ca}, one may complete the contour integration over $\partial S_\triangle$ in Eq. (A.1) and, arrive at the closed-form solution

for $\mathcal{I}_{00}$,

$$\mathcal{I}_{00}(z, S_\triangle) = \sum_{n=0}^{5} \frac{i^n k^{n-1}}{n!} \sum_{m=0}^{n} \frac{(-1)^{n-m} n!}{m!(n-m)!} \Big\{ e^{ikr_\circ^{ab}} (r_\circ^{ab})^{n-m} I_{ms}(z, a, b)$$
$$+ e^{ik\,r_\circ^{bc}} (r_\circ^{bc})^{n-m} I_{ms}(z, b, c)$$
$$+ e^{ik\,r_\circ^{ca}} (r_\circ^{ca})^{n-m} I_{ms}(z, c, a) \Big\}, \quad z \notin S_\triangle \quad \text{(A.4)}$$

where $s = -1$, $r_\circ^{bc}$ and $r_\circ^{ca}$ are described – similar to $r_\circ^{ab}$ definition – as

$$r_\circ^{bc} = \left| z - \tau_\circ^{bc} \right|, \quad \tau_\circ^{bc} = \frac{b+c}{2}, \quad r_\circ^{ca} = \left| z - \tau_\circ^{ca} \right|, \quad \tau_\circ^{ca} = \frac{a+c}{2}. \quad \text{(A.5)}$$

Recall that I_{ms} is precisely defined by Eq. (22) whereby the following recursive identities are extracted for $s = -1$:

$$I_{2s}(z,a,b) = h^2 I_{0s}(z,a,b) + 2\overline{d}(b-a) + D_{ab} I_{01}(z,a,b),$$
$$I_{3s}(z,a,b) = h^2 I_{1s}(z,a,b) + 2\overline{d} I_{10}(z,a,b) + D_{ab} I_{11}(z,a,b),$$
$$I_{4s}(z,a,b) = h^4 I_{0s}(z,a,b) + 4\overline{d}h^2(b-a) + (4\overline{d}^2 + 2h^2 D_{ab}) I_{01}(z,a,b)$$
$$+ 4\overline{d}D_{ab} I_{02}(z,a,b) + D_{ab}^2 I_{03}(z,a,b),$$
$$I_{5s}(z,a,b) = h^4 I_{1s}(z,a,b) + 4\overline{d}h^2 I_{10}(z,a,b) + (4\overline{d}^2 + 2h^2 D_{ab}) I_{11}(z,a,b)$$
$$+ 4\overline{d}D_{ab} I_{12}(z,a,b) + D_{ab}^2 I_{13}(z,a,b). \quad \text{(A.6)}$$

It is apparent that a and b in the expressions of Eq. (A.6) are dummy variables, and these expressions are valid for any straight segment. It must be mentioned that the integrals I_{0q} with $q \geq -1$ are regarded as known as they only involve integration of basic functions e.g. polynomials. Moreover, the integral I_{1s} ($s = -1$) is provided by Eq. (23), and the integrals I_{1q} for $q \geq 0$ can be found in Eqs. (8.8)–(8.11) of [14]. This completes the construction of the analytical expression for the integral $\mathcal{I}_{00}$ of Eq. (A.4).

Analytical solution of $\mathcal{I}_{11}(z, S_\triangle)$ and $\mathcal{I}_{22}(z, S_\triangle)$: The integral $\mathcal{I}_{mn}$ is computed (for $m = n = 1, 2$) following similar steps as in Eqs. (A.1)–(A.4), resulting in the analytical expressions presented below:

$$\mathcal{I}_{11}(z, S_\triangle) = \int_{S_\triangle} \frac{|\tau - z|^2}{r} e^{ikr} \, dS_\triangle = \frac{1}{k^3} \Big\{ \mathcal{A}_0 k\, \mathcal{I}_{00}(z, S_\triangle) + \sum_{\sigma=1}^{2} \mathcal{A}_\sigma \int_{\partial S_\triangle} \frac{r^\sigma}{\tau - z} e^{ikr} \, d\tau \Big\}, \quad z \notin S_\triangle,$$

$$\mathcal{I}_{22}(z, S_\triangle) = \int_{S_\triangle} \frac{|\tau - z|^4}{r} e^{ikr} \, dS_\triangle = \frac{1}{k^5} \Big\{ \mathcal{B}_0 k\, \mathcal{I}_{00}(z, S_\triangle) + \sum_{\sigma=1}^{4} \mathcal{B}_\sigma \int_{\partial S_\triangle} \frac{r^\sigma}{\tau - z} e^{ikr} \, d\tau \Big\}, \quad z \notin S_\triangle,$$
$$\text{(A.7)}$$

where

$$\mathcal{A}_0 = -k^2 h^2 - 2, \quad \mathcal{A}_1 = 2ik, \quad \mathcal{A}_2 = k^2, \quad \mathcal{B}_0 = 24 + 4k^2 h^2 + k^4 h^4,$$
$$\mathcal{B}_1 = -4ik(6 + h^2 k^2), \quad \mathcal{B}_2 = -2k^2(6 + h^2 k^2), \quad \mathcal{B}_3 = 4ik^3, \quad \mathcal{B}_4 = k^4. \quad \text{(A.8)}$$

By invoking expansions of Eqs. (21) and (A.3), the contour integral in Eq. (A.7) is analytically evaluated as follows:

$$\int_{\partial S_\triangle} \frac{r^\sigma}{\tau - z} e^{ikr} \, d\tau = \sum_{n=0}^{5} \frac{i^n k^n}{n} \sum_{m=0}^{n} \frac{(-1)^{n-m} n!}{m!(n-m)!} \Big\{ e^{ik\,r_\circ^{ab}} (r_\circ^{ab})^{n-m} I_{(m+\sigma)s}(z, a, b)$$
$$+ e^{ik\,r_\circ^{bc}} (r_\circ^{bc})^{n-m} I_{(m+\sigma)s}(z, b, c) + e^{ik\,r_\circ^{ca}} (r_\circ^{ca})^{n-m} I_{(m+\sigma)s}(z, c, a) \Big\},$$
$$\times (s = -1, \sigma \geq 1). \quad \text{(A.9)}$$

It is straightforward to generalize Eq. (A.6) to obtain recursive formulae for the integrals I_{qs} for $s = -1$, $q \geq 5$. For instance, the case I_{6s} is illustrated below:

$$I_{6s}(z,a,b) = h^6 I_{0s}(z,a,b) + 6\overline{d}h^4(b-a) + (12\overline{d}^2\,h^2$$
$$+ 3h^4 D_{ab}) I_{01}(z,a,b) + (12\overline{d}h^2 D_{ab} + 8\overline{d}^3)$$
$$\times I_{02}(z,a,b) + (12\overline{d}^2\,D_{ab} + 3h^2 D_{ab}^2) I_{03}(z,a,b)$$
$$+ 6\overline{d}D_{ab}^2 I_{04}(z,a,b) + D_{ab}^3 I_{05}(z,a,b). \quad \text{(A.10)}$$

That completes the integrations of Eq. (A.7).

For the cases under consideration, appropriate free terms should be added to expressions in Eq. (A.4) when $z \in S_\triangle$ or,

$z \in \partial S_\triangle$. These terms are

$$m = n = 0 : \begin{cases} \dfrac{2\pi i}{k}\, e^{ik|h|}, & z \in S \\[2mm] \dfrac{\gamma i}{k}\, e^{ik|h|}, & z \in \partial S \end{cases} \quad \text{(A.11)}$$

The corresponding terms for Eq. (A.7) are

$$m = n = 1 : \begin{cases} \dfrac{4\pi i}{k^3}\, e^{ik|h|}(ik|h| - 1), z \in S \dfrac{2\gamma i}{k^3}\, e^{ik|h|}(ik|h| - 1), z \in \partial S \end{cases}$$

$$m = n = 2 : \begin{cases} \dfrac{16\pi i}{k^5}\, e^{ik|h|}(3 - 3ik|h| - k^2 h^2), z \in S \dfrac{8\gamma i}{k^5}\, e^{ik|h|}(3 - 3ik|h| - k^2 h^2), z \in \partial S \end{cases}$$
$$\text{(A.12)}$$

where γ is defined in Eq. (13).

A.2. Analytical integration of $\mathcal{I}_{mn}(z, S_\circ)$

This section provides closed-form expressions affiliated with the integrals of Fig. 4 and Table 2. Analytical solution of the integral $\mathcal{I}_{mn}(z, S_\circ)$ over the circular sector $S_\circ$ illustrated in Fig. 1(c) is simply achieved by replacing $S_\triangle$ by $S_\circ$ in Eqs. (A.1) and (A.7), e.g. for $m = n = 1$,

$$\mathcal{I}_{11}(z, S_\circ) = \int_{S_\circ} \frac{|\tau - z|^2}{r} e^{ikr} \, dS_\circ = \frac{1}{k^3} \Big\{ \mathcal{A}_0 k\, \mathcal{I}_{00}(z, S_\circ) + \sum_{\sigma=1}^{2} \mathcal{A}_\sigma \int_{\partial S_\circ} \frac{r^\sigma}{\tau - z} e^{ikr} \, d\tau \Big\}, \quad z \notin S_\circ.$$
$$\text{(A.13)}$$

These equations stem from Eqs. (12) and (15), as demonstrated in the first part of A.1. The crucial part, however, is to describe the contour integral

$$\int_{\partial S_\circ} \frac{r^\sigma}{\tau - z} e^{ikr} \, d\tau, \quad \sigma = 0, 1, \ldots, 4. \quad \text{(A.14)}$$

By invoking the asymptotic expansion equation (21) and the binomial theorem of Eqs. (A.3), one arrives at the following:

$$\int_{\partial S_\circ} \frac{r^\sigma}{\tau - z} e^{ikr} \, d\tau = \sum_{n=0}^{5} \frac{i^n k^n}{n!} \sum_{m=0}^{n} \frac{(-1)^{n-m} n!}{m!(n-m)!} \Big\{ e^{ik\,r_\circ^{ab}} (r_\circ^{ab})^{n-m} I_{(m+\sigma)s}(z, a, b)$$
$$+ e^{ik\,r_\circ^{bc}} (r_\circ^{bc})^{n-m} J_{(m+\sigma)s}(z, b, c) + e^{ik\,r_\circ^{ca}} (r_\circ^{ca})^{n-m} I_{(m+\sigma)s}(z, c, a) \Big\},$$
$$\times (s = -1, \sigma \geq 0). \quad \text{(A.15)}$$

wherein $r_\circ^{\widehat{bc}} = |z - \tau_\circ^{\widehat{bc}}|$ defined for circular segment $\widehat{bc}$, with $\tau_\circ^{\widehat{bc}}$ being the mid-arc point shown in Fig. 1(c); $J_{qs}(z, b, c)$ is introduced by Eqs. (26)–(27) whose solution for $q = 1$ is given by Eq. (33), and for $q = 0$ is considered as known due to the elementary nature of its corresponding integral. In cases where $q \geq 1$, recursive equations are used in the same fashion as described by Eqs. (A.6) and (A.10), i.e.

$$J_{2s}(z,a,b) = h^2 J_{0s}(z,a,b) + (\overline{z}_c - \overline{z})(b-a) + R^2 J_{0s}(z_c,a,b),$$
$$J_{3s}(z,a,b) = h^2 J_{1s}(z,a,b) + (\overline{z}_c - \overline{z}) J_{10}(z,a,b) + R^2 J_{1s}(z_c,a,b),$$
$$J_{4s}(z,a,b) = h^4 J_{0s}(z,a,b) + 2(h^2 + R^2)(\overline{z}_c - \overline{z})(b-a) + R^2(R^2 + 2h^2$$
$$+ 2|z_c - z|^2) J_{0s}(z_c,a,b) + (\overline{z}_c - \overline{z})^2 J_{01}(z,a,b) + R^4(z_c - z) J_{0(s-1)}(z_c,a,b),$$

$$J_{5s}(z,a,b) = h^4 J_{1s}(z,a,b) + 2(h^2 + R^2)(\overline{z}_c - \overline{z}) J_{10}(z,a,b) + R^2(R^2 + 2h^2$$
$$+ 2|z_c - z|^2) J_{1s}(z_c,a,b) + (\overline{z}_c - \overline{z})^2 J_{11}(z,a,b) + R^4(z_c - z) J_{1(s-1)}(z_c,a,b),$$
$$\text{(A.16)}$$

derived using Eq. (26). Recall that for $s = -1$, the integral $J_{1(s-1)}$ is given by Eq. (34). Furthermore, the integrals J_{10} and, J_{11} can be found in Eqs. (8.17)–(8.21) of [14]. It should be mentioned that $J_{qs}(z, b, c)$ for $q \geq 6$ can be expressed in the same recursive manner.

References

[1] Bonnet M. Boundary integral equation methods for solids and fluids. Chichester: John Wiley & Sons; 1999.

[2] Carini A, Salvadori A. Analytical integrations in 3D BEM: preliminaries. Comput Mech 2002;28:177–85.

[3] Carley M. Analytical formulae for potential integrals on triangles. J Appl Mech 2013;80:041008.

[4] Dassios G, Kleinman R. Low frequency scattering. Oxford: Clarendon Press; 2000.

[5] Gaul L, Kgl M, Wagner M. Boundary element methods for engineers and scientists. An introductory course with advanced topics. Berlin: Springer; 2003.

[6] Gradshteyn IS, Ryzhik IM. Table of integrals, series, and products. 6th edition. San Diego: Academic Press; 2000.

[7] Hsiao GC, Wendland WL. Boundary integral equations. Berlin: Springer-Verlag; 2008.

[8] Lenoir M, Salles N. Evaluation of 3-D singular and nearly singular integrals in Galerkin BEM for thin layers. SIAM J Sci Comput 2012;34:3057–78.

[9] Linkov AM. Boundary integral equations in elasticity theory. Dordrecht, Netherlands: Kluwer Academic Publishers; 2002.

[10] Linkov AM, Mogilevskaya SG. Complex hypersingular BEM in plane elasticity problems; 1998.

[11] Liu Y. Fast multipole boundary element method: theory and applications in engineering. Cambridge: Cambridge University Press; 2009.

[12] Medina DE, Ligget JA. Exact integrals for three-dimensional boundary element potential problems. Commun Appl Numer Methods 1989;5:555–61.

[13] Mogilevskaya SG. The universal algorithm based on complex hypersingular integral equation to solve plane elasticity problems. Comput Mech 1996;18:127–38.

[14] Mogilevskaya SG, Nikolskiy DV. The use of complex integral representations for analytical evaluation of three dimensional BEM integrals – potential and elasticity problems. Q J Mech Appl Math 2014;67:505–23.

[15] Nintcheu Fata S. Explicit expressions for 3D boundary integrals in potential theory. Int J Numer Methods Eng 2009;78:32–47.

[16] Nintcheu Fata S. Semi-analytic treatment of nearly-singular Galerkin surface integrals. Appl Numer Math 2010;60:974–93.

[17] Nintcheu Fata S. Explicit expressions for three-dimensional boundary integrals in linear elasticity. J Comput Appl Math 2011;235:4480–95.

[18] Okon EE, Harrington RF. The potential integral for a linear distribution over a triangular domain. Int J Numer Methods Eng 1982;18:1821–8.

[19] Pompeiu D. Sur une classe de functions d'une variable complexe et sur certaine equations integrales. Rend Circ Mat Palermo 1913;35:277–81.

[20] Rjasanow S, Steinbach O. The fast solution of boundary integral equations. Berlin: Springer; 2007.

[21] Salvadori A. Analytical integrations of hypersingular kernel in 3D BEM problems. Comput Methods Appl Mech Eng 2001;190:3957–75.

[22] Salvadori A. Analytical integrations in 2D BEM elasticity. Int J Numer Methods Eng 2002;53:1695–719.

[23] Salvadori A. Analytical integrations in 3D BEM for elliptic problems: evaluation and implementation. Int J Numer Methods Eng 2010;84:505–42.

[24] Salvadori A, Temponi A. Analytical integrations for the approximation of 3D hyperbolic scalar boundary integral equations. Eng Anal Bound Elem 2010;34:977–94.

[25] Tadeu A, Antonio J. 3D acoustic wave simulation using BEM formulations: closed form integration of singular and hypersingular integrals. Eng Anal Bound Elem 2012;36:1389–96.

[26] Tadeu A, Prata J, Simoes N. Closed form integration of singular and hypersingular integrals in 3D BEM formulations for heat conduction. Math Prob Eng 2012:647038.

[27] Vekua IN. Generalized analytic functions. Oxford: Pergamon Press; 1962.

[28] Wu H, Liu Y, Jiang W. Analytical integration of the moments in the diagonal form fast multipole boundary element method for 3-D acoustic wave problems. Eng Anal Bound Elem 2012;36:248–54.